

## Video Article

# An Invasive Method for the Activation of the Mouse Dentate Gyrus by High-frequency Stimulation

Zhe Zhao<sup>1</sup>, Haitao Wu<sup>1,2</sup><sup>1</sup>Department of Neurobiology, Beijing Institute of Basic Medical Sciences<sup>2</sup>Key Laboratory of Neuroregeneration, Co-innovation Center of Neuroregeneration, Nantong UniversityCorrespondence to: Haitao Wu at [wuht@bmi.ac.cn](mailto:wuht@bmi.ac.cn)URL: <https://www.jove.com/video/57857>DOI: [doi:10.3791/57857](https://doi.org/10.3791/57857)

Keywords: Neuroscience, Issue 136, High-frequency, stimulation, dentate gyrus, neuronal activity, neurogenesis, BrdU labeling

Date Published: 6/2/2018

Citation: Zhao, Z., Wu, H. An Invasive Method for the Activation of the Mouse Dentate Gyrus by High-frequency Stimulation. *J. Vis. Exp.* (136), e57857, doi:10.3791/57857 (2018).

## Abstract

Electrical high-frequency stimulation (HFS), using implanted electrodes targeting various brain regions, has been proven as an effective treatment for various neurological and psychiatric disorders. HFS in the deep region of the brain, also named deep-brain stimulation (DBS), is becoming increasingly important in clinical trials. Recent progress in the field of high-frequency DBS (HF-DBS) surgery has begun to spread the possibility of utilizing this invasive technique to other situations, such as treatment for major depression disorder (MDD), obsessive-compulsive disorder (OCD), and so on.

Despite these expanding indications, the underlying mechanisms of the beneficial effects of HF-DBS remain enigmatic. To address this question, one approach is to use implanted electrodes that sparsely activate distributed subpopulations of neurons by HFS. It has been reported that HFS in the anterior nucleus of the thalamus could be used for the treatment of refractory epilepsy in the clinic. The underlying mechanisms might be related to the increased neurogenesis and altered neuronal activity. Therefore, we are interested in exploring the physiological alterations by the detection of neuronal activity as well as neurogenesis in the mouse dentate gyrus (DG) before and after HFS treatment.

In this manuscript, we describe methodologies for HFS to target the activation of the DG in mice, directly or indirectly and in an acute or chronic manner. In addition, we describe a detailed protocol for the preparation of brain slices for *c-fos* and Notch1 immunofluorescent staining to monitor the neuronal activity and signaling activation and for bromodeoxyuridine (BrdU) labeling to determine the neurogenesis after the HF-DBS induction. The activation of the neuronal activity and neurogenesis after the HF-DBS treatment provides direct neurobiological evidence and potential therapeutic benefits. Particularly, this methodology can be modified and applied to target other interested brain regions such as the basal ganglia and subthalamic regions for specific brain disorders in the clinic.

## Video Link

The video component of this article can be found at <https://www.jove.com/video/57857/>

## Introduction

HF-DBS is a neurosurgical technology for electrical stimulation in the brain, which has been developed since the 1870s<sup>1</sup>. In the late 1980s, HFS was first used as a potential therapeutic intervention for Parkinson's disease and other movement disorders<sup>2</sup>. In the past few decades, HF-DBS has been more and more widely used in the treatment of brain disorders which are currently untreatable by a traditional therapeutic strategy. Particularly, due to the accuracy improvement of the HFS electrode, the highly effective outcomes, and minimal side effects, the number of brain disorders treated by HF-DBS has significantly increased over the past decades<sup>3,4,5</sup>. For example, HF-DBS has been approved by the US Food and Drug Administration (FDA) for the treatment of Parkinson's disease (PD), Alzheimer's type dementia, essential tremor, and other types of movement disorders<sup>2,6,7</sup>. In PD patients, the dopaminergic medication is reduced up to 50% during HF-DBS<sup>8</sup>. In addition to the successful treatment of movement disorders, HF-DBS has also demonstrated its powerful effects in the treatment of psychiatric diseases in the clinic, and for cognitive augmentation as well<sup>2,9,10,11</sup>. It should be noted that the research of HFS for the treatment of other psychiatric disorders are in various stages, offering much promise to patients<sup>12</sup>.

Although many studies have demonstrated that a focal HFS has both local and remote effects throughout the brain<sup>13</sup>, the neurological and molecular mechanisms of the effects remain elusive<sup>2,14</sup>. In the clinic, therapeutic HF-DBS is usually applied in a long-term manner for the treatment of Parkinson's disease and chronic pain, *etc.* Many opinions are raised to explain the improvement generated by an HF-DBS treatment, among which one possibility that the HFS current modulates the neuronal network activity, probably by a repetitive depolarization of the axons in the vicinity of the implanted HFS electrode. Or, HF-DBS may change the discharge rate of the output neurons and the projected targets. Also, HF-DBS may lead to long-term synaptic changes, including long-term potentiation (LTP) and long-term depression (LTD), which may contribute to a symptomatic improvement. So far, it is still unclear whether HFS influences the key molecular events that regulate cellular processes such as adult neurogenesis *in vivo*. Several lines of studies have demonstrated that HFS in rodents could mimic similar neural responses of clinically applied DBS<sup>15,16</sup>. To understand the underlying cellular mechanisms of HF-DBS, in this study, we first set up an *in vivo*

HFS methodology in mice in an acute (one day) or chronic (five days) manner. Secondly, we set up an activation analysis methodology to determine the alteration of the neuronal activity and neurogenesis after an HF-DBS delivery.

Given that the neuronal production from neural stem cells is abundant during the embryonic development but continues throughout adult life, the hippocampal subgranular zone is one of the major areas where the neurogenesis occurs. The process of neurogenesis is influenced by many physiological and pathological factors. In certain epileptic cases, the hippocampal neurogenesis is dramatically decreased<sup>17,18</sup>. In addition, a single electroconvulsive therapy could significantly increase the neuronal production in the dentate gyrus<sup>19</sup>. These observations suggest that the electrophysiological activity plays a critical role in the regulation of adult neurogenesis and synaptic plasticity in hippocampal neurons. Therefore, to further demonstrate the effects of HF-DBS on neuronal activity and neurogenesis, we first carry out an immunostaining assay of the immediate early gene (IEG) *c-fos* which is a well-known marker of short-term neuronal activity resulting from experience<sup>20</sup>. Notch1 signaling is also detected to monitor the signaling activation after the HFS delivery<sup>21,22</sup>. Moreover, we also detect the neuronal production by a BrdU labeling analysis after the HF-DBS induction in various manners, though BrdU staining can also be a marker for gliogenesis.

In the present study, two HFS methodologies are adapted to target the activation of the hippocampal DG directly and indirectly. The electrode is implanted into the DG directly or implanted into the medial perforant path (PP) which sends projections to activate the DG neurons. For the HF-DBS induction, a programmable stimulator is presented for a continuous stimulation *via* the fixed electrode onto the mouse head. To determine the effects of HFS on neuronal activation and neurogenesis, we detect the expression of *c-fos* and Notch1 by immunofluorescent staining and the number of BrdU-incorporated positive neurons in the hippocampal DG region, respectively, after the HFS treatment. Particularly, the effects of the HF-DBS on the neurogenesis in the DG are compared between an acute and a chronic stimulation manner, or between a direct and an indirect stimulation manner, respectively.

## Protocol

Animal experimental procedures followed the institutional guidelines of the Beijing Institute of Basic Medical Sciences (Beijing, China) and the Chinese governmental regulations for the Care and Use of Laboratory Animals. The mice (adult male, 26 ~ 30 g) were housed and kept at a constant temperature of 23 °C, with water and food *ad libitum*, under a 12-h light/12-h dark cycle (lights on at 7:00 a.m.). All experimental procedures were performed during the light cycle.

### 1. Surgical Preparation

NOTE: A custom electrode was homemade using the method modified from Halpern's report<sup>23</sup>.

1. Use 2 copper micro-wires (with an outer diameter of 200  $\mu\text{m}$ ) as the parallel bipolar electrode. Wrap the electrodes around each other to form cylindrical electrodes for the stimulation.  
NOTE: Here, the electrode length within either the PP or DG was varied according to the anatomical depth of the nucleus.
2. Sterilize the electrodes using an Ethylene oxide disinfection cabinet. Handle and store the homemade 2-channel micro-wire electrodes without any contamination. The electrodes should be strictly sterilized before any surgical implantation.
3. Autoclave the surgical instruments.
4. Before the surgery, inject the mouse with pentobarbital (20 - 50 mg/kg) intraperitoneally, to achieve a surgical plane of anesthesia.
5. Inject the mouse with a sterile penicillin G procaine suspension (75,000 U, I.M.) and an analgesic agent (carprofen, 0.05 - 1 mg/kg, SC) to decrease the risk of infections and pain, respectively<sup>24</sup>.
6. After the animal anesthesia, apply an eye lubricant to both eyes to prevent eye dryness. Ensure the induction of the sedation and the depth of the anesthesia by the animal's reflexes in response to toe pinching and proceed with the operation only when no response occurs.  
NOTE: Vet ointment is another option to prevent eye dryness.
7. Shave most of the fur on the top of the mouse head with electrical hair clippers or a razor blade, sterilize the shaved area with three alternating scrubs of 70% alcohol and betadine solution and proceed with the operation after the betadine has dried on the skin.

### 2. High-Frequency Stimulation Surgery<sup>25,26</sup>

NOTE: In this step, an electrode is unilaterally implanted into the dorsal DG or medial PP area, a part of the hippocampus with critical roles in episodic learning and memory.

1. Place the anesthetized mouse onto the stereotactic frame. To keep the mouse's head immobile, align the ear bars properly and install them quickly. Gently tighten the ear bars so that they support the centered head and secure the mouse slightly.
2. Use a thermostatic pad to maintain the animal's body temperature at  $37 \pm 0.5$  °C.
3. Use forceps to grasp the skin anterior to the mouse ears and cut it with sterilized scissors to remove about 1-cm<sup>2</sup> area of skin on the top of the mouse's skull.  
NOTE: A small amount of bleeding could be observed along the edges of the cut skin.
4. Remove the muscle and other attachment overlying the skull with a cotton swab to expose the skull surface. Use a cotton swab and dissecting chisel to clean all periosteum, tendons and connective tissue from the skull's surface completely to identify the sagittal and lambda sutures lines.
5. Identify the bregma and lambda point. The intersection of the coronal suture and the sagittal suture on the superior middle portion of the calvaria is where the bregma is located. The intersection of the lambdoid suture by the sagittal suture is where the lambda is visible. Use the bregma as the original point to set the other nucleus position.
6. After the identification of the bregma and lambda position on the skull, adjust these two points in the horizontal level. Make sure that the height of these two points is almost the same in the dorsal-ventral direction (any errors should be < 0.05 mm). Also, make sure that the skull is level in the medial-lateral direction in the same way<sup>26</sup>.

7. For a unilateral surgery, mount a homemade 2-channel copper micro-wire electrode into the rotating electrode holder on the stereotactic surgical frame.
8. Place the electrode vertically above the bregma point at first, and set it as original site. Use the digital displayed stereotactic surgical frame to indicate the anterior-posterior (AP), medial-lateral (ML), and dorso-ventral (DV) positions.  
NOTE: To prevent the electrode from getting bent, do not touch the electrode tip onto the skull during the operation.
9. Move the electrode gently to the correct position (**Figure 1A**, AP-2.1/ML  $\pm$  1.0 for DG and AP-3.8/ML  $\pm$  3.0 for PP, respectively)<sup>27</sup> above the skull without any touch. When the desired site was identified for electrode insertion, use the dorsoventral stereotactic adjustments to higher the electrodes holder, and mark the position with a black marker.  
NOTE: The exact location in reference to the stereotaxic coordinates may vary by mouse strain, weight, and sex. Adult mice of the same sex should be used to minimize any variation in the location. If possible, pre-operational anatomical scans should be used to identify the location on an individual subject basis<sup>27</sup>.
10. Use a hand-held micromanipulator-assisted drill (burr size = 0.5 mm) to make burr holes at the marked position precisely. Sterilize the tip of the burr with 70% ethanol before drilling. Move up the mini drill bit through the skull along the Z-axis 0.8 - 1.0 mm without changing its X-Y position. Use a sterile cotton to stop any bleeding during the operation.  
NOTE: To avoid over-drilling and excessive heat generation during the drilling, ensure the drilling speed is 15,000 - 18,000 revolutions per minute (RPM), and frequently withdraw the drill bit from burr hole every 8 - 10 s.
11. Keep drilling until the dura is exposed. Use a bent needle to remove any bone scraps that are generated during the drilling and make a pinhole on the dura without damaging the underlying soft brain tissue.  
NOTE: To avoid damaging the brain tissue, the bent blunt needle can also be replaced with a fine blunt forceps.
12. To confirm that the burr holes have been made properly at the desired position, reduce the electrode height by an adjustment of the stereotactic surgery frame and ensure that the electrode can be inserted smoothly through the burr hole without touching any obstacles. If so, slowly insert the electrodes to a depth of 1.8 mm for the DG (or 3.0 mm for the PP) from the surface of the skull located at the medial PP to the DG (PP-DG).  
NOTE: Wipe off any cerebrospinal fluid or blood outflows from the burr holes with sterile cotton during the process of the electrode implantation.
13. After inserting the micro-wire electrode into the skull hole, hold it in place with adequate dental cement using a small spatula. As the cement thickens, mold it around the inserted electrode and screws to form a nice smooth cap. Debride and disinfect the wound edges.
14. Disengage the electrode from the electrode holder. Remove the mouse from the stereotactic frame and return it to a warm cage.  
NOTE: After surgery, wait with returning the animals to their cages until they have fully recovered from the anesthesia with sufficient consciousness.
15. Let the mouse move freely and allow it to recover for 2 days in the cage. Then, connect the electrode implanted in the mouse brain to a programmable stimulator *via* leads. Set up the software interface as presented in **Figure 2**. Set the HFS parameters as 6 series of 6 trains of 6 pulses at 400 Hz (**Figure 1B**, 100 ms between the trains, 20 s between the series)<sup>28</sup>. Set the stimulation intensity to 200  $\mu$ A.
16. Deliver an HFS for the desired period of time as set up. Deliver the stimulation 2x a day at 8:00 a.m. and at 8:00 p.m.
17. For the control group, implant electrodes in the mice and do not perform a stimulation.
18. For the *c-fos* staining, stimulate the experimental mice acutely (2x per day). For the BrdU labeling, divide the experimental mice into an acute stimulation group (applied 2x per day) and a chronic stimulation group (applied 10x in 5 days, 2x per day). During the course of the stimulation, make sure the mouse is awake. Remember to ensure the leads are not twisted.  
NOTE: At the last day of the procedure, the mice in the acute stimulation group were stimulated simultaneously.
19. When the stimulation is done, carefully disconnect the electrode pin from the electrode holder and the connector of the recording system.

### 3. Immunofluorescence Staining and Bromodeoxyuridine Labeling<sup>29</sup>

1. For the *c-fos* and Notch1 staining, about 3 h after the last HF-DBS stimulation, anesthetize the mice by injecting pentobarbital (20 - 50 mg/kg, I.P.) to achieve a surgical plane of anesthesia.
2. For the BrdU labeling, about 12 h after the last HF-DBS stimulation, give 6 injections of BrdU to the control and the stimulated mice at 2-h intervals (50 mg/kg in 0.9% saline, I.P.). 36 h after the last injection, anesthetize the mice by injecting pentobarbital (20 - 50 mg/kg, I.P.) to achieve a surgical plane.
3. Make incisions using a scalpel through the rib cage to expose the heart and then pass a 22-gauge blunt perfusion needle to the left ventricle. Make a small incision in the right atrium. Transcardially perfuse it with 50 mL of cold phosphate-buffered saline (PBS) followed by 50 mL of cold 4% paraformaldehyde (PFA) in 1x PBS (pH 7.4).  
NOTE: Switch the PBS to the PFA when the mouse blood *in vivo* is replaced and the fluid runs clear. A good perfusion can be judged by the clearing of the liver. The perfusion should be stopped once fixation tremors have been observed<sup>30</sup>.
4. Decapitate the mouse with ophthalmic scissors, make an incision on the skin and expose the skull. Using forceps, chip off the skull slightly and carefully dissect the whole mouse brain. Post-fix the brain in 4% paraformaldehyde for an additional 2 days and transfer it to a 30% sucrose solution at 4 °C overnight.
5. Using a cryostat, cut the brains into 20- $\mu$ m coronal sections. Transfer and mount the sections to the glass slide with a brush and store them at -20 °C.  
NOTE: Animals with electrode misplacements or excessive mechanical damage will be excluded from the subsequent analysis.
6. Transfer the slides into normal PBS (0.1 M, pH 7.4) containing no fixative. Wash the slices with PBS for 3 - 4x for 5 min each to remove any excess fixative. For the BrdU-labeled group, incubate the sections in 2-N HCl for 30 min at 37 °C, and rinse them in a 0.1-M borate buffer (pH 8.4; 10 min). Then wash the slices 2x for 5 min in PBS.  
NOTE: Immunostaining is then performed.
7. Treat slices by incubation in blocking solution (1 % normal goat serum, 3 % bovine serum albumin <BSA>, 0.5 % Triton X-100 and 0.02 % sodium azide in 1 x PBS) for 1 h at room temperature (RT).
8. Incubate the slices with anti-*c-fos* polyclonal antibody (1:500; rabbit), anti-Notch1 antibody (1:50; goat), or anti-BrdU antibody (1:800; rat) in the blocking solution at 4 °C overnight.
9. Wash the slices 3x in PBS, then incubate them with Alexa Fluor 568-conjugated anti-rabbit (1:500), Alexa Fluor 488-conjugated anti-goat (1:1,000), or Alexa Fluor 488-conjugated anti-rat (1:500) secondary antibody for 1 h at RT.

10. Wash the samples 3x in PBS (10 min each time). Cover the immuno-labeled brain sections using an anti-fade reagent mounting medium containing DAPI. Let the slices air-dry and store them protected from light at 4 °C.
11. Acquire images of the hippocampal areas from the stimulated and unstimulated sides of the brain with a high-resolution multi-channel (sequential) scanning confocal microscope. Set the imaging parameters consistently between the control and experimental groups.
12. Perform a mosaic imaging using a high-magnification objective (20X air objective, NA 0.45) to acquire continuous 3D (XYZ) images of adjacent fields of view using the motorized stage and utilize appropriate software to stitch them together to make large composite images. NOTE: Tiling functions include true stitching and smoothing options for improved seamless images. Composite images are quickly and easily prepared using the stitching function, to form an image over a wide area.
13. For *c-fos* and Notch1 staining, perform a positive nuclei quantitative analysis of the immunofluorescent density<sup>21</sup> of the stitched images. Randomly select 3 areas in the rostral, dorsal, and ventral hippocampal DG subregions and measure the immunofluorescent density in a double-blinded manner using **Image J** software (<http://rsb.info.nih.gov/ij/>)<sup>31</sup>.
14. For a BrdU labeling, analyze the slices around the drilling point through the dorsal hippocampus (-1.7 mm to -2.7 mm relative to the bregma) in a double-blinded manner.
15. Count only BrdU-positive neurons in the DG. Include the cells lying within 2-cell diameters of the granule cell in the count. NOTE: Here, counting was performed using a 40X air objective. Randomly, 3 - 5 sections per animal were counted, and the counts were averaged and expressed as means per DG<sup>19</sup>.

## Representative Results

Following the HF-DBS stimulation to the hippocampal DG subregion directly or the PP subregion to activate the DG indirectly *via* inserted electrodes using the stereotactic adjustments, the rodents were anesthetized with pentobarbital and sampled 3 h after the last HF-DBS stimulation for the *c-fos* and Notch1 immunostaining. For the BrdU staining, 36 h after the last BrdU injection after 1 day or 5 days of HF-DBS stimulation, the rodents were anesthetized with pentobarbital for the preparation of brain sections. **Figure 3** shows that the expression of *c-fos* was significantly increased in the ipsilateral side of the DG. In addition, the *c-fos* expression in the contralateral side of the DG was also upregulated compared to the no-HF-DBS stimulation controls who showed almost no expression of a *c-fos* signal. Based on the Notch1-specific immunofluorescent staining in brain slices, as shown in **Supplementary Figure 1**, we further demonstrated that the Notch1 signaling could also be activated in the adult hippocampal DG after the HFS stimulation by an induction of the depolarization of neurons in the PP (also refer to the raw data supplied as **Supplementary File 1**).

In addition to the direct HF-DBS stimulation in the DG subregion, **Figure 4A** shows the position and the HF-DBS stimulation site of the electrode tip, which was installed in the medial PP. **Figure 4B** demonstrated that the HF-DBS stimulation in the PP not only significantly increased the level of the *c-fos* expression in the ipsilateral side of the DG, but also increased the expression of *c-fos* in the contralateral side of the DG compared to the no-HF-DBS stimulation controls.

Based on the BrdU labeling analysis of the brain slices, as shown in **Figures 5A - 5C**, we further demonstrated that neurogenesis can also be activated in the adult hippocampal DG after a chronic (5 days) HF-DBS stimulation in the DG directly. A chronic HF-DBS stimulation in the DG not only significantly upregulated the neurogenesis in the ipsilateral side but also increased the neurogenesis in the contralateral side compared to the no-HF-DBS stimulation controls. However, the acute (1 day) stimulation failed to induce an upregulation of the neurogenesis either in ipsilateral side or in the contralateral side of the DG. As shown in **Figure 5D**, either in the acute stimulation group or in the chronic stimulation group, an indirect HF-DBS in the PP could not change the neurogenesis level in the hippocampal DG.

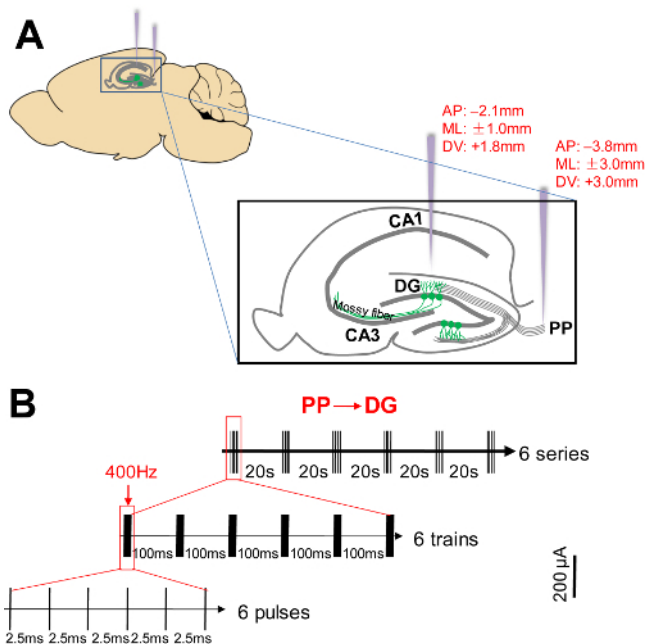


**Figure 1. Schematic representation of the brain targets of the electrode tip and parameters of the HFS.** (A) The neuronal projection of the medial perforant path into an inferior blade of the dentate gyrus is indicated. The position of the inserted electrodes (in purple) to stimulate either the DG directly or the PP subregion are indicated. (B) The HFS parameter is indicated as 6 series of 6 trains of 6 pulses at 400 Hz, with 100 ms between the trains and 20 s between the series. CA = the Cornu Ammonis; DG = the dentate gyrus; PP = the perforant path. [Please click here to view a larger version of this figure.](#)

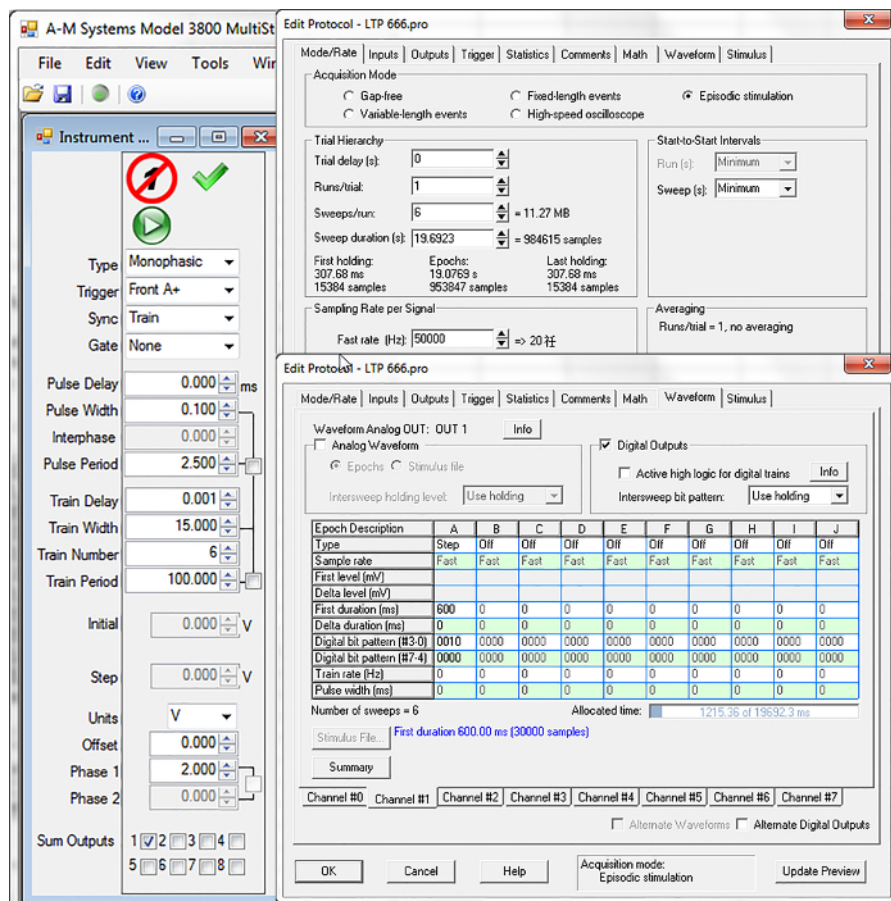


**Figure 2. Interface and parameters of the multistimulator.** The stimulator was connected to a digital-analog converter and activated by proprietary software. The stimulus type of the HFS was monophasic. [Please click here to view a larger version of this figure.](#)



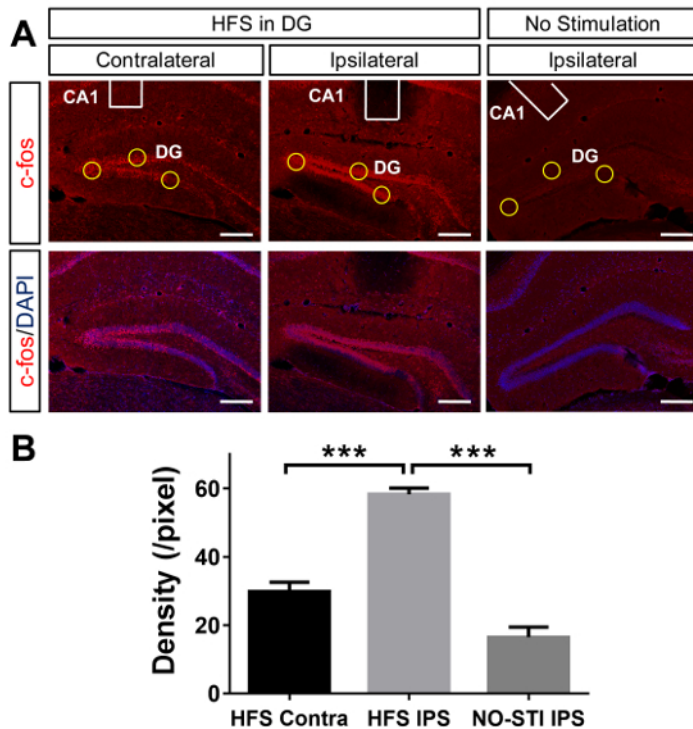


**Figure 3. Neuronal activation in the DG in response to the HF-DBS treatment directly.** (A) The electrode tip (the white unfilled box) was positioned above the DG region directly (AP -2.1/ML ±1.0/ DV +1.8) with or without the HFS. This panel shows the immunostaining of the coronal section of the brain slices with a *c-fos* antibody in the control and the HFS groups. DAPI blue staining was used to indicate the location of the hippocampal nuclei. The scale bar = 100 μm. (B) This panel shows a quantitative analysis of the immunofluorescence signal density. In the ipsilateral side of the DG, the neurons were significantly activated with a high expression of *c-fos*, and the *c-fos* expression in the contralateral side of the DG is also relatively increased compared to the *c-fos* expression of control mice without an HFS treatment. Means ± SEM, one-way ANOVA,  $F_{2,24} = 216$ ,  $P < 0.0001$ , Bonferroni *post hoc* test,  $***P < 0.001$ ,  $n_{no-sti} = 9$  (3 slices from 3 mice),  $n_{HFS\ Contra} = 9$  (3 slices/mouse from 3 mice),  $n_{HFS\ IPS} = 9$  (3 slices/mouse from 3 mice). [Please click here to view a larger version of this figure.](#)

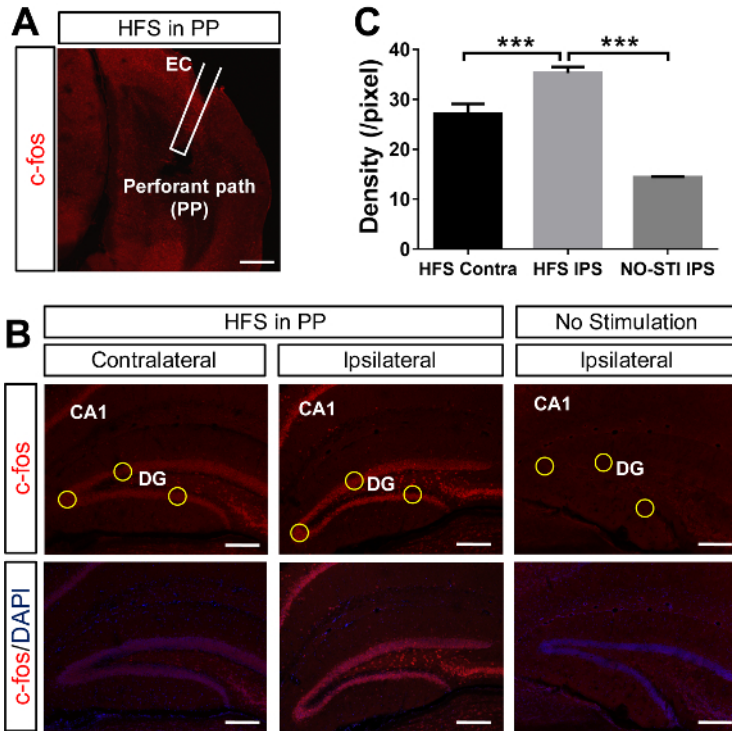


**Figure 4. Neuronal activation in the DG in response to the HFS in the PP subregion.** (A) The electrode tip (the white unfilled box) was positioned in the medial PP at the position of AP -3.8, ML ±3.0, and DV +3.0, with or without the HFS. (B) This panel shows the immunostaining of the coronal section of the brain slices with *c-fos* antibody in the control and the HFS groups. DAPI blue staining was used to indicate the location of the hippocampal nuclei. The scale bar = 100 μm. (C) This panel shows a quantitative analysis of the immunofluorescent density. The HFS treatment in the PP could significantly activate ipsilateral neurons in the DG with a high expression of *c-fos*. The expression of *c-fos* in the contralateral DG is also relatively increased compared to the *c-fos* expression of the control mice without an HFS treatment. Means ± SEM, one-way ANOVA,  $F_{2,24} = 189.3$ ,  $P < 0.0001$ , Bonferroni *post hoc* test,  $***P < 0.001$ ,  $n_{no-sti} = 9$  (3 slices from 3 mice),  $n_{HFS\ Contra} = 9$  (3 slices/mouse from 3 mice),  $n_{HFS\ IPS} = 9$  (3 slices/mouse from 3 mice). [Please click here to view a larger version of this figure.](#)

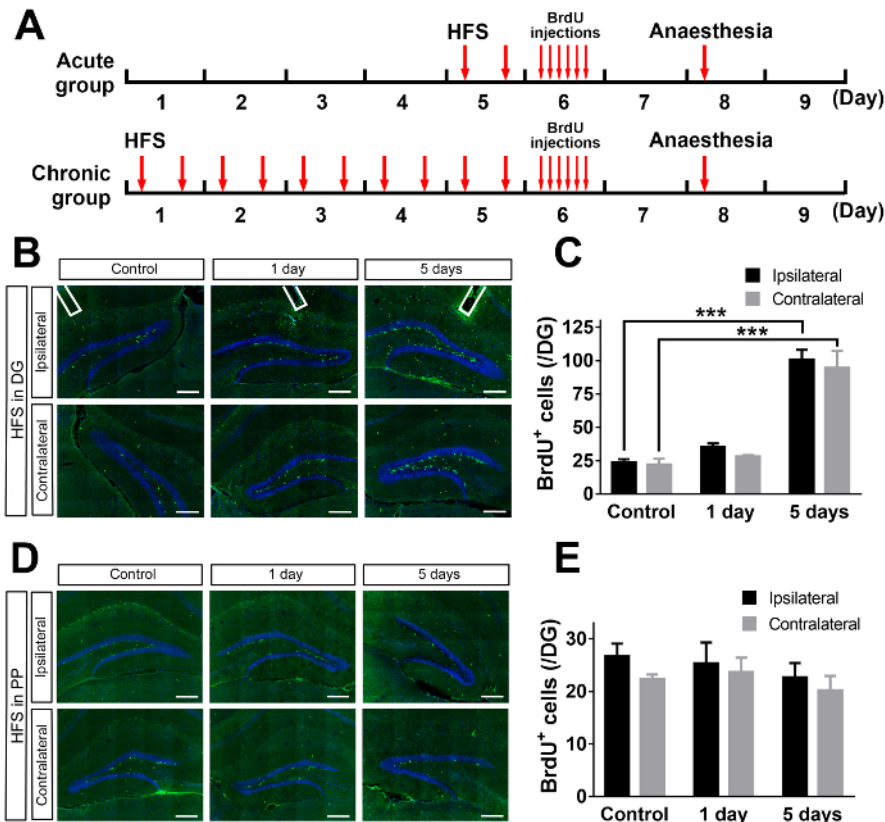
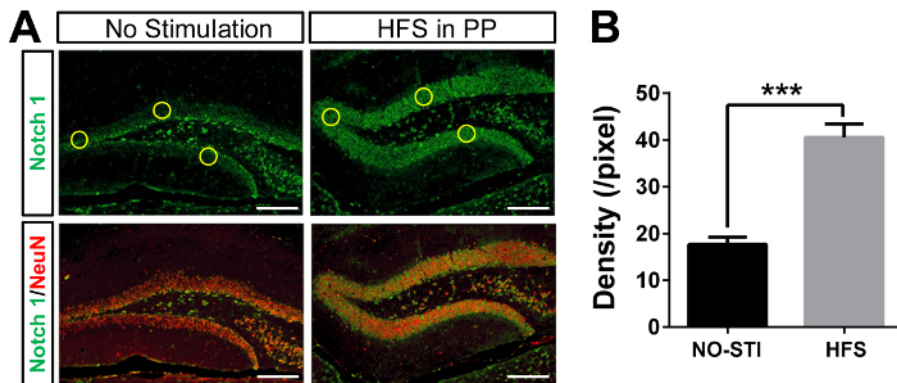


**Figure 5. Distinct activation of neurogenesis in the DG in response to HFS in DG and PP respectively.** (A) This panel shows an experimental paradigm for the HFS treatment and the generation of BrdU-labeled proliferating neurons in the DG. The animals were divided into an acute and a chronic group. In the acute group, the mice were subjected to an HFS treatment 2x on day 5. In the chronic group, the mice were subjected to an HFS treatment for 5 days (from day 1 to day 5, 2x per day). Then, the animals in both groups were injected with BrdU (50 mg/kg, 6x by 2-h intervals) on day 6. On day 8, the animals were anesthetized and perfused for the preparation of cryostat sections. (B) This panel shows the immunofluorescent staining of BrdU (in green) post-HF-DBS in the DG. (C) A quantitative analysis of the neuronal production indicated that the acute (2x in 1 day) stimulation in the DG could not enhance the neurogenesis, while the chronic (10x within 5 days) stimulation in the DG significantly upregulated the neurogenesis. Compared to the control group, the number of BrdU labeling cells increased significantly in the chronic group both in the ipsilateral and contralateral hemisphere. The scale bar = 100  $\mu$ m. Means  $\pm$  SEM, two-way ANOVA, stimulation type effect  $F_{2, 14} = 97.09$ ,  $P < 0.0001$ , hemisphere effect  $F_{1, 14} = 1.137$ ,  $P = 0.3044$ , Bonferroni *post hoc* test,  $***P < 0.001$ ,  $n_{\text{Control}} = 3$  (3 slices from 3 mice),  $n_{1 \text{ day}} = 4$  (4 slices from 3 mice),  $n_{5 \text{ days}} = 3$  (3 slices from 3 mice). (D) This panel shows the immunofluorescence staining of BrdU (in green) post-HF-DBS in the PP subregion. (E) A quantitative analysis of the neuronal production indicated that either the acute (twice in one day) or chronic (10x in 5 days) stimulation in the PP could not enhance the neurogenesis significantly. The number of BrdU labeling cells was relatively stable with or without the HFS treatment. The scale bar = 100  $\mu$ m. Means  $\pm$  SEM, two-way ANOVA, stimulation type effect  $F_{2, 16} = 0.9025$ ,  $P = 0.4252$ , hemisphere effect  $F_{1, 16} = 1.402$ ,  $P = 0.2537$ , Bonferroni *post hoc* test,  $P > 0.05$ ,  $n_{\text{Control}} = 3$  (3 slices from 3 mice),  $n_{1 \text{ day}} = 3$  (3 slices from 3 mice),  $n_{5 \text{ days}} = 5$  (5 slices from 3 mice). [Please click here to view a larger version of this figure.](#)





**Supplementary Figure 1. Expression of Notch1 in the DG in response to HF-DBS treatment.** (A) This panel shows the immunofluorescent staining of Notch1 (in green) 3 h after the HF-DBS in the DG. This figure was cited and modified from Feng's report<sup>21</sup>. (B) A quantitative analysis of the fluorescence indicated that the HFS in the DG could enhance the expression of Notch1. The scale bar = 100  $\mu$ m. Means  $\pm$  SEM, student *t*-test, *t* = 12, \*\*\**P* < 0.001, *n*<sub>no-sti</sub> = 9 (3 slices/mouse from 3 mice), *n*<sub>HFS</sub> = 9 (3 slices/mouse from 3 mice). [Please click here to view a larger version of this figure.](#)

DBS/PP DBS CNL	Stim	Area (Pixel)	Intensity (Pixel/mm <sup>2</sup> )	Mean (Pixel)	SD (Pixel)
DBS/PP DBS CNL 1	1	200	4076	20.3812500	1.9112500
	2	200	3108	15.5400000	1.4100000
	3	200	3744	18.7200000	1.6200000
DBS/PP DBS CNL 2	4	200	4336	21.6800000	2.0600000
	5	200	3168	15.8400000	1.4400000
	6	200	3768	18.8400000	1.6800000
DBS/PP DBS CNL 3	7	200	4400	22.0000000	2.0000000
	8	200	4720	23.6000000	2.1600000
	9	200	4800	24.0000000	2.2000000
PP DBS CNL 1	1	200	4016	20.0800000	1.8080000
	2	200	3640	18.2000000	1.7200000
	3	200	4200	21.0000000	1.9000000
PP DBS CNL 2	4	200	3640	18.2000000	1.7200000
	5	200	3640	18.2000000	1.7200000
	6	200	3720	18.6000000	1.7600000
PP DBS CNL 3	7	200	4240	21.2000000	1.9200000
	8	200	4320	21.6000000	1.9600000
	9	200	4320	21.6000000	1.9600000

**Supplementary File 1. Raw Data.** [Please click here to download this file.](#)

## Discussion

The HF-DBS technique has been widely used as a powerful tool for the treatment of many neurological disorders since the 1990s. So far, the landmark work of HF-DBS is for the treatment of Parkinson's disease and essential tremor, which has attracted much attention and interest both in the clinic and scientific community. There are various types of ongoing HF-DBS studies by many groups for HF-DBS's therapeutic application in certain neurological and psychiatric disorders<sup>32,33</sup>. Some of these studies are currently in various stages of clinical trials<sup>2,34</sup>. Although HF-DBS should bring significant benefit, stimulation side effects can occur even with a perfect placement in the brain, such as negative changes in mood and thinking, *etc.*, which are reversible and can be avoided with modifications of the stimulation settings.

In addition to the significant progress of the HF-DBS technology accumulated from the clinical trials over the past decades, the studies of HF-DBS in live animals also presents the opportunity to understand the physiological changes and neurobiological mechanisms induced by the electrical stimulation. In this manuscript, we have described a modified HF-DBS methodology performed in mice to stimulate the hippocampal DG subregion with an HFS directly or indirectly. Although the described protocol is performed in rodents, HFS response studies have also been successfully conducted in other model organisms, including pigs<sup>35</sup>. For this technique, stereotactic surgery can also be used for a potential nucleus-targeted stimulation to test out the efficacy of the HFS using certain animal models with neurological and psychiatric disorders. The conclusions drawn from such studies should readily translate to the clinic, specifically for the refinement of the HFS at existing targets. Note that in contrast to the series of multiple exposures of HF-DBS in the clinic, in this methodological study, we chose a single and short-term exposure of HFS to stimulate and induce the neuronal activity in the hippocampal DG, the parameter and part of the paradigm of HFS that was previously reported to induce LTP in the hippocampus slices<sup>21,28</sup>.

General limitations of HF-DBS have been extensively reviewed elsewhere<sup>24,25</sup>. One of the challenges for the experiment here is also the need for an excellent surgical technique and for the ongoing care of surgical anatomical locus. To correctly and precisely implant the electrode into the target nucleus for stimulation, one of the key processes is a successful surgery by a skilled technician to avoid unnecessary blood vessel injury and the misplacement of the electrode. Moreover, further anatomical and histological analysis of the brain specimen is also needed to confirm the proper targeting of the electrode after an HFS. This is also one of the advantages of this approach, to clearly demonstrate the corrected targeting of the electrode after the operation in an intact animal brain. Many of the details provided in this protocol can be readily adapted for a long-term stimulation *via* an implanted stimulator in the animal. It should be noted that it is also amenable to alternate stimulation parameters in potential therapeutic brain targets with different HFS delivery patterns. However, this article reported on a single-unit acute HFS delivered by a programmable stimulator unit to understand the cellular changes after the electrical stimulation.

Although HF-DBS serves as an alternative option for the treatment of neurological and psychiatric disorders in the clinic for several years, the mechanisms underlying its effectiveness remain poorly understood. Considering the use and future improvements of HF-DBS, a more pragmatic approach is required. As a developing tool, the HFS technique needs further technical innovation and mechanistic discovery. To study the cellular and molecular mechanisms of HF-DBS, a global transcriptome analysis based on high-throughput sequencing technologies will provide important information to understand the molecular events and signaling changes after an HF-DBS induction<sup>36</sup>. In addition to the unbiased

screening strategy, based on the examination of existing molecular candidates which have been proven to respond to neuronal depolarization, it will probably also provide important clues to identify the key effectors responsible for HFS with. *C-fos* is upregulated in response to intrinsic neuronal activity, so looking at its expression would at least provide us a landscape of neurons fired recently<sup>37</sup>. However, *c-fos* should not only be used to just reflect activities since it also appears to mark neurons undergoing LTP<sup>37</sup>. Previous works, including ours, have demonstrated that Notch1 plays a critical role in the synaptic plasticity in mature hippocampal neurons and is essential for adult neurogenesis *in vivo*<sup>21,22</sup>. In terms of this situation, a detailed quantitative and spatiotemporal localization of key candidates should be carefully characterized and described pre- and post-HFS induction by an immunohistochemical analysis of the *c-fos* expression. Studies like this will provide direct evidence to demonstrate the changes of gene expression patterns in various brain regions in response to an HFS<sup>21</sup>, which will also be beneficial to reveal the cellular changes such as neuronal activation, neurogenesis, or neurodegeneration.

It should also be noted that despite the advantages of an HF-DBS application in the clinic, due to the fact that the outcomes of the stimulation effect are tightly associated with the stimulation parameters and target location in the brain, the cellular and molecular mechanisms underlying HFS's effects might be very complicated. In this study, we further carried out BrdU labeling to investigate the acute and chronic effects of HFS on adult neurogenesis. Although BrdU staining can be a marker for both neurogenesis and gliogenesis, based on previous reports, the majority of increased BrdU positive neurons observed at the SGZ after an HF-DBS treatment should be the proliferative adult neural progenitors<sup>21,38,39</sup>. Regardless of the complexity of the mechanisms underlying the HFS treatment, the methods and results we described in this manuscript provide direct evidence that repetitive high-frequency electrical stimulation to activate the hippocampal DG could significantly induce the activation of neuronal activity and neurogenesis *in vivo*.

In summary, we demonstrated that an HF-DBS can improve the neuronal activity and neurogenesis of mice, compared to the neuronal activity and neurogenesis of control mice who did not undergo an HF-DBS. This may advance the scientific understanding regarding cognitive effects and stimulation patterning of HFS *in vivo*. The identification of neuronal activation after an acute HF-DBS treatment directly or indirectly *in vivo* demonstrates that an HFS treatment has significant effects on the synaptic transmission of local and long-range connections. The rapid induction of neuronal activation after an HF-DBS treatment provides a powerful tool to manipulate the impaired synaptic transmission or desynchronization in many neurological and psychiatric disorders such as MDD. On the other hand, the induction of neurogenesis after a chronic and direct, but not acute or indirect HF-DBS treatment suggests the distinct efficacy and functional variability between different electrical stimulation manners. Such findings provide direct evidence for the neural modulation and potential therapeutic benefits of HFS in the future. Taken together, HF-DBS will present substantial advantages for the treatment of neurological and psychiatric disorders by integrating the technological advances made in the clinic and the mechanistic progress made in the laboratory.

## Disclosures

The authors have nothing to declare.

## Acknowledgements

Supported by the National Natural Science Foundation of China Grants 31522029, 31770929 and 31371149 (to Haitao Wu), Program 973 (2014CB542203) from the State Key Development Program for Basic Research of China (to Haitao Wu), and Grant Z161100000216154 from the Beijing Municipal Science and Technology Commission (to Haitao Wu). The authors thank all the members of the Haitao Wu laboratory for their encouragement and discussions. The authors are extremely grateful to Zhenwei Liu for his help with debugging the apparatus.

## References

- Perlmutter, J. S., Mink, J. W. Deep brain stimulation. *Annual Review of Neuroscience*. **29** 229-257 (2006).
- Lozano, A. M., Lipsman, N. Probing and regulating dysfunctional circuits using deep brain stimulation. *Neuron*. **77** (3), 406-424 (2013).
- Kohl, S. *et al.* Deep brain stimulation for treatment-refractory obsessive compulsive disorder: a systematic review. *BMC Psychiatry*. **14**, 214 (2014).
- Schlaepfer, T. E., Bewernick, B. H., Kayser, S., Madler, B., Coenen, V. A. Rapid effects of deep brain stimulation for treatment-resistant major depression. *Biological Psychiatry*. **73** (12), 1204-1212 (2013).
- Fisher, R. *et al.* Electrical stimulation of the anterior nucleus of thalamus for treatment of refractory epilepsy. *Epilepsia*. **51** (5), 899-908 (2010).
- Greenberg, B. D. *et al.* Deep brain stimulation of the ventral internal capsule/ventral striatum for obsessive-compulsive disorder: worldwide experience. *Molecular Psychiatry*. **15** (1), 64-79 (2010).
- Kalia, S. K., Sankar, T., Lozano, A. M. Deep brain stimulation for Parkinson's disease and other movement disorders. *Current Opinion in Neurology*. **26** (4), 374-380 (2013).
- Garcia, L., D'Alessandro, G., Bioulac, B., Hammond, C. High-frequency stimulation in Parkinson's disease: more or less? *Trends in Neurosciences*. **28** (4), 209-216 (2005).
- Guercio, L. A., Schmidt, H. D., Pierce, R. C. Deep brain stimulation of the nucleus accumbens shell attenuates cue-induced reinstatement of both cocaine and sucrose seeking in rats. *Behavioural Brain Research*. **281**, 125-130 (2015).
- Bossert, J. M., Marchant, N. J., Calu, D. J., Shaham, Y. The reinstatement model of drug relapse: recent neurobiological findings, emerging research topics, and translational research. *Psychopharmacology*(Berlin). **229** (3), 453-476 (2013).
- Grubert, C. *et al.* Neuropsychological safety of nucleus accumbens deep brain stimulation for major depression: effects of 12-month stimulation. *The World Journal of Biological Psychiatry*. **12** (7), 516-527 (2011).
- Lyons, M. K. Deep brain stimulation: current and future clinical applications. *Mayo Clinic Proceedings*. **86** (7), 662-672 (2011).
- McIntyre, C. C., Hahn, P. J. Network perspectives on the mechanisms of deep brain stimulation. *Neurobiology of Disease*. **38** (3), 329-337 (2010).

14. Kringelbach, M. L., Green, A. L., Owen, S. L., Schweder, P. M., Aziz, T. Z. Sing the mind electric - principles of deep brain stimulation. *European Journal of Neuroscience*. **32** (7), 1070-1079 (2010).
15. Toda, H., Hamani, C., Fawcett, A. P., Hutchison, W. D., Lozano, A. M. The regulation of adult rodent hippocampal neurogenesis by deep brain stimulation. *Journal of Neurosurgery*. **108** (1), 132-138 (2008).
16. Selvakumar, T., Alavian, K. N., Tierney, T. Analysis of gene expression changes in the rat hippocampus after deep brain stimulation of the anterior thalamic nucleus. *Journal of Visualized Experiments*. (97), e52457 (2015).
17. Hattiangady, B., Shetty, A. K. Implications of decreased hippocampal neurogenesis in chronic temporal lobe epilepsy. *Epilepsia*. **49** Suppl 5, 26-41 (2008).
18. Hattiangady, B., Rao, M. S., Shetty, A. K. Chronic temporal lobe epilepsy is associated with severely declined dentate neurogenesis in the adult hippocampus. *Neurobiology of Disease*. **17** (3), 473-490 (2004).
19. Madsen, T. M. *et al.* Increased neurogenesis in a model of electroconvulsive therapy. *Biological Psychiatry*. **47** (12), 1043-1049 (2000).
20. Feldman, L. A., Shapiro, M. L., Nalbantoglu, J. A novel, rapidly acquired and persistent spatial memory task that induces immediate early gene expression. *Behavioral and Brain Functions*. **6**, 35 (2010).
21. Feng, S. *et al.* Notch1 deficiency in postnatal neural progenitor cells in the dentate gyrus leads to emotional and cognitive impairment. *The FASEB Journal*. **31** (10), 4347-4358 (2017).
22. Alberi, L. *et al.* Activity-induced Notch signaling in neurons requires Arc/Arg3.1 and is essential for synaptic plasticity in hippocampal networks. *Neuron*. **69** (3), 437-444 (2011).
23. Halpern, C. H., Attiah, M. A., Tekriwal, A., Baltuch, G. H. A step-wise approach to deep brain stimulation in mice. *Acta Neurochirurgica(Wien)*. **156** (8), 1515-1521 (2014).
24. Batra, V., Guerin, G. F., Goeders, N. E., Wilden, J. A. A General method for evaluating deep brain stimulation effects on intravenous methamphetamine self-administration. *Journal of Visualized Experiments*. (107), e53266 (2016).
25. Fluri, F., Bieber, M., Volkman, J., Kleinschnitz, C. Microelectrode guided implantation of electrodes into the subthalamic nucleus of rats for long-term deep brain stimulation. *Journal of Visualized Experiments*. (104), e53066 (2015).
26. Resendez, S. L. *et al.* Visualization of cortical, subcortical and deep brain neural circuit dynamics during naturalistic mammalian behavior with head-mounted microscopes and chronically implanted lenses. *Nature Protocols*. **11** (3), 566-597 (2016).
27. Paxinos, G., Franklin, K. The mouse brain in stereotaxic coordinates, 3rd edition. *The Mouse Brain in Stereotaxic Coordinates*. **28** (03), 6 (2007).
28. McHugh, T. J. *et al.* Dentate gyrus NMDA receptors mediate rapid pattern separation in the hippocampal network. *Science*. **317** (5834), 94-99 (2007).
29. Gonzalez, C. *et al.* Medial prefrontal cortex is a crucial node of a rapid learning system that retrieves recent and remote memories. *Neurobiology of Learning and Memory*. **103**, 19-25 (2013).
30. Gage, G. J., Kipke, D. R., Shain, W. Whole animal perfusion fixation for rodents. *Journal of Visualized Experiments*. (65), e3564 (2012).
31. Tse, N. *et al.* The neuromuscular junction: measuring synapse size, fragmentation and changes in synaptic protein density using confocal fluorescence microscopy. *Journal of Visualized Experiments*. (94), e52220 (2014).
32. Pizzolato, G., Mandat, T. Deep brain stimulation for movement disorders. *Frontiers in Integrative Neuroscience*. **6**, 2 (2012).
33. Tierney, T. S., Sankar, T., Lozano, A. M. Some recent trends and further promising directions in functional neurosurgery. *Acta Neurochirurgica Supplement*. **117** (117), 87-92 (2013).
34. Laxton, A. W. *et al.* A phase I trial of deep brain stimulation of memory circuits in Alzheimer's disease. *Annals of Neurology*. **68** (4), 521-534 (2010).
35. Min, H. K. *et al.* Deep brain stimulation induces BOLD activation in motor and non-motor networks: an fMRI comparison study of STN and EN/GPi DBS in large animals. *NeuroImage*. **63** (3), 1408-1420 (2012).
36. Kukurba, K. R., Montgomery, S. B. RNA sequencing and analysis. *Cold Spring Harbor Protocols*. **2015** (11), 951-969 (2015).
37. Kawashima, T., Okuno, H., Bito, H. A new era for functional labeling of neurons: activity-dependent promoters have come of age. *Frontiers in Neural Circuits*. **8**, 37 (2014).
38. Liu, J., Solway, K., Messing, R. O., Sharp, F. R. Increased neurogenesis in the dentate gyrus after transient global ischemia in gerbils. *Journal of Neuroscience*. **18** (19), 7768-7778 (1998).
39. Kuhn, H. G., Dickinson-Anson, H., Gage, F. H. Neurogenesis in the dentate gyrus of the adult rat: age-related decrease of neuronal progenitor proliferation. *Journal of Neuroscience*. **16** (6), 2027-2033 (1996).